



Direct evidence of a prey depletion “halo” surrounding a pelagic predator colony

Sam B. Weber^{a,b,1}, Andrew J. Richardson^b, Judith Brown^b, Mark Bolton^c, Bethany L. Clark^{a,d}, Brendan J. Godley^a, Eliza Leat^b, Steffen Oppel^c, Laura Shearer^b, Karline E. R. Soetaert^e, Nicola Weber^{a,b}, and Annette C. Broderick^a

^aCentre for Ecology and Conservation, University of Exeter, Penryn, Cornwall TR10 9FE, United Kingdom; ^bAscension Island Government Conservation and Fisheries Department, Georgetown, Ascension Island ASCN 1ZZ, United Kingdom; ^cCentre for Conservation Science, Royal Society for the Protection of Birds, Sandy, Bedfordshire SG19 2DL, United Kingdom; ^dBirdLife International, Cambridge CB2 3QZ, United Kingdom; and ^eDepartment of Estuarine and Delta Systems, Royal Netherlands Institute for Sea Research, 4400 AC, Yerseke, The Netherlands

Edited by James A. Estes, University of California, Santa Cruz, CA, and approved May 19, 2021 (received for review January 29, 2021)

Colonially breeding birds and mammals form some of the largest gatherings of apex predators in the natural world and have provided model systems for studying mechanisms of population regulation in animals. According to one influential hypothesis, intense competition for food among large numbers of spatially constrained foragers should result in a zone of prey depletion surrounding such colonies, ultimately limiting their size. However, while indirect and theoretical support for this phenomenon, known as “Ashmole’s halo,” has steadily accumulated, direct evidence remains exceptionally scarce. Using a combination of vessel-based surveys and Global Positioning System tracking, we show that pelagic seabirds breeding at the tropical island that first inspired Ashmole’s hypothesis do indeed deplete their primary prey species (flying fish; *Exocoetidae* spp.) over a considerable area, with reduced prey density detectable >150 km from the colony. The observed prey gradient was mirrored by an opposing trend in seabird foraging effort, could not be explained by confounding environmental variability, and can be approximated using a mechanistic consumption–dispersion model, incorporating realistic rates of seabird predation and random prey dispersal. Our results provide a rare view of the resource footprint of a pelagic seabird colony and reveal how aggregations of these central-place foraging, marine top predators profoundly influence the oceans that surround them.

Ashmole’s halo | central-place foraging | predator–prey interaction | seabird | competition

By consuming, harassing, and intimidating their prey, top predators can radically affect the abundance and distribution of species at lower trophic levels (1–5), which, in turn, can regulate predator numbers (6–9). Classic population dynamic models predict that as the local density of a predator increases, per capita prey availability will fall either because prey is depleted or increasingly take steps to avoid or evade capture. However, despite their fundamental importance in ecology, such interactions are often extremely difficult to quantify directly. Typically, some form of manipulation or perturbation of predator numbers is needed before the scale of their impacts on food webs become apparent (4, 10), and, even then, measuring how prey responds is rarely straightforward. This is particularly true in the open ocean where both predators and prey may be elusive and widely dispersed over vast areas (5).

Aggregations of colonially breeding seabirds and marine mammals have long provided model systems for studying food-limited, density-dependent population regulation in animals (6–9, 11) and may provide rare opportunities to directly observe the impacts of marine apex predators on their prey base (12). Not only can such colonies be exceptionally large (>1 million individuals in extreme cases), most colonial breeders are also central-place foragers and are constrained in the distance they can travel in search of food by the need to periodically return to their nests or nurseries to care for dependent young. All the

resources needed to sustain the reproduction of large numbers of individuals must therefore be extracted from a confined area located within commuting range of the colony. In his seminal work on population regulation in seabirds, Ashmole (7) hypothesized that the resulting concentration of foraging effort would drive localized prey depletion in accessible foraging areas surrounding large predator colonies, forcing individuals to travel ever further afield in search of food. As colonies grow, he reasoned, so too would the prey-depleted zone, until eventually population growth stalls through density-dependent reductions in provisioning rates and breeding success.

Ashmole’s hypothesis has a strong theoretical basis and can be framed as an optimal foraging problem in which individual colony members attempt to maximize their net rate of energy gain (13). For central-place foragers, the time and energy expended accessing a food patch increases as a function of distance traveled from the colony. Capture rates and/or prey quality must therefore be correspondingly higher at more distant sites in order to achieve the same marginal energetic return. Through the collective rate-maximizing behavior of large numbers of individuals, prey availability is reduced such that the energetic return that can be derived from all potential foraging locations is equalized (the “ideal free distribution”), manifesting as opposing gradients of increasing prey availability and decreasing predator density with distance traveled from the colony (13).

Significance

Elucidating the mechanisms that regulate animal populations is a fundamental goal in ecology and is increasingly important at a time of unprecedented anthropogenic disturbance to ecosystems. Here, we present direct evidence of a phenomenon known as “Ashmole’s halo”: a zone of prey depletion that is hypothesized to form around aggregations of central-place foraging predators and is believed to be the principal mechanism regulating populations of many colonially breeding animals. In effect, Ashmole’s halo constitutes rare, visible evidence of the food limitation that naturally limits many predator populations and can be exacerbated by human impacts such as fisheries. Therefore, the large extent of the resource footprint we demonstrate has important implications for conservation of marine food webs at ecologically relevant scales.

Author contributions: S.B.W., J.B., B.J.G., and A.C.B. designed research; S.B.W., A.J.R., J.B., M.B., B.L.C., E.L., S.O., L.S., and N.W. performed research; S.B.W. and K.E.R.S. analyzed data; and S.B.W., A.J.R., J.B., M.B., B.L.C., B.J.G., E.L., S.O., L.S., K.E.R.S., N.W., and A.C.B. wrote the paper.

The authors declare no competing interest.

This article is a PNAS Direct Submission.

Published under the [PNAS license](#).

¹To whom correspondence may be addressed. Email: sam.weber@exeter.ac.uk.

This article contains supporting information online at <https://www.pnas.org/lookup/suppl/doi:10.1073/pnas.2101325118/-DCSupplemental>.

Published July 6, 2021.

This theoretical prey gradient is commonly referred to as “Ashmole’s halo” (12) and has been highly influential in shaping our understanding of the population dynamics, behavior, and life histories of seabirds (6, 8, 11–14) and other colonial central-place foragers [e.g., seals (9), raptors (15), and human fishers (16)]. However, almost six decades since it was proposed, direct evidence that such “halos” form in nature is extremely scarce. In the marine realm, the best evidence remains the study of Birt et al. (12), who showed that the abundance of demersal fish in four temperate, coastal bays declined within close proximity of nearby cormorant colonies (although without controlling for confounding environmental variability between sites). Ainley et al. also provided corroborating evidence by demonstrating that the vertical distribution (and hence availability) of prey schools around seabird colonies varies as a function of colony size (17) and seasonally increasing foraging intensity (18) but were unable to detect the predicted gradient in prey availability with distance traveled from the colony. Given the challenges of directly quantifying prey distributions around marine predator colonies, support for Ashmole’s halo has instead been largely inferred from correlations between measures of foraging efficiency (e.g., foraging range, diet quality, and breeding success) and proxies of prey availability (e.g., colony size, stage in breeding season, and interspecific competition) (6, 19–24). However, while such relationships are logically consistent with prey depletion, they are largely phenomenological, and alternative explanations can often be invoked to explain them (13).

To provide unambiguous evidence of Ashmole’s halo, it is necessary to show that prey abundance in comparable habitats increases as a function of distance from the colony and that this trend arises due to lower predator density. Here, we construct such a test at the Ascension Island seabird colony that first inspired Ashmole’s hypothesis (7) using simultaneous estimates of predator and prey abundance gathered during >2,800 km of ship-based surveys carried out throughout the Island’s 200-nautical-mile exclusive economic zone. Ascension Island is typical of many seabird colonies in hosting populations of multiple species with overlapping diets (~1 million individuals belonging to 11 species) (25) but is located in an otherwise featureless part of the Atlantic Ocean where prey densities are unlikely to be affected by neighboring colonies (14), making it an ideal location to search for Ashmole’s halo.

Our test of Ashmole’s hypothesis consists of three steps. First, we consider how overall seabird densities observed in at-sea surveys relate to the distribution of an important shared prey resource. Next, using a multispecies Global Positioning System (GPS) tracking dataset containing >300 foraging trips undertaken by the three most abundant large-bodied seabirds, we validate foraging distributions for breeding (i.e., colony-constrained) birds and show how the behavior of individual colony members influences, and is influenced by, the observed prey distribution. Finally, we explore the mechanistic basis for Ashmole’s halo using a simple consumption–dispersion model that incorporates data from at-sea surveys and tracking to simulate the effects of seabird predation on mobile, pelagic prey. Together, the results provide compelling evidence for the existence of Ashmole’s halo and its origins in the central-place foraging of colonially breeding predators.

Results and Discussion

Predator–Prey Surveys. Like many tropical oceanic seabirds, the diets of larger-bodied seabird species nesting on Ascension Island consist of a high proportion of flying fish (26–28), which was corroborated by regurgitate samples collected opportunistically throughout the study: Flying fish were present in 67 to 95% of spontaneous regurgitates obtained from nesting masked boobies *Sula dactylatra* ($n = 21$), brown boobies *Sula leucogaster* ($n = 9$), and Ascension frigatebirds *Fregata aquila* ($n = 26$)

between 2014 and 2020 and were the most frequently observed prey item (*SI Appendix, Table S1* and *SI Appendix*). To investigate how this important shared prey resource is distributed around the colony, established visual census techniques were used to simultaneously estimate the relative abundance of seabirds and flying fish along 192 fixed duration transects (mean length = 14.5 ± 3.2 km; Fig. 1 and *SI Appendix, Table S2*) coinciding with seasonal breeding peaks over four consecutive years (*SI Appendix, Fig. S1*). Seabird counts were dominated by species that breed on Ascension along with a small proportion (~1.5%) of nonbreeding oceanic migrants (*SI Appendix, Table S3*). An estimated 14,652 flying fish were also observed across all surveys. We could not reliably differentiate between flying fish species in flight and present total counts throughout; however, identification of a sample of individuals that landed on the deck of the survey vessel ($n = 43$) indicated that tropical two-winged flying fish (*Exocoetus volitans*) were particularly common (85%), with smaller numbers of *Cheilopogon pinnatibarbus* (8%), *Prognichthys glaphyrae* (5%), and *Hirundichthys speculiger* (3%) making up the remainder (*SI Appendix, Table S4*). This ratio corresponds well with that in the diets of seabirds nesting on Ascension, with *E. volitans* predominating (26–28).

The survey method used to enumerate flying fish primarily targets adults (29), which was reflected in the estimated life stages of the individuals counted (ca. 96% adult) and in measurements taken from the deck strike sample (mean total length = 19.7 cm; *SI Appendix, Table S4*). Of the seabird species breeding on Ascension, only boobies (*Sula* spp.), Ascension frigatebirds, and tropicbirds (*Phaethon* spp.) routinely predate adult flying fish in this size class (27, 28, 30). To provide a relevant comparison with observed prey densities, we therefore calculated overall seabird abundance for each transect by pooling counts of these larger-bodied species, 97.6% of which consisted of the three dominant species represented in our dietary sampling (Ascension frigatebirds, masked boobies, and brown boobies) (*SI Appendix, Table S3*). Within transects, flying fish occurred in discrete “patches” (*SI Appendix, Fig. S2*), resulting in counts that were significantly spatially aggregated (Lloyd’s Patchiness index: mean = 3.7 [95% CI: 3.4 to 4.1], where 1 represents a random, Poisson distribution). Thus, in addition to calculating the overall abundance of flying fish for each survey, a series of “patch metrics” were also derived to quantify the number, mean size, and mean density of prey patches encountered.

Direct Evidence of Ashmole’s Halo at Ascension Island. Generalized additive (mixed) models (GAM(M)s) fit to at-sea survey data explained 70% and 44% of the deviance in seabird and flying fish counts, respectively. Consistent with Ashmole’s hypothesis, of the 16 explanatory variables tested, distance from Ascension Island was by far the strongest predictor of abundance in both models (Table 1), with directly opposing trends; total abundance of seabirds increased with greater proximity to the island, and this trend was mirrored by a corresponding decrease in the density of their flying fish prey (Fig. 1). Estimated pointwise CIs around the first derivatives of the fitted GAM(M) splines indicate that flying fish density was depressed up to 220 km from the colony (Fig. 2 and *SI Appendix, Fig. S3*), increasing from an average of 0.5 individuals \cdot km⁻¹ (95% CI = 0.3 to 0.8) at a distance of 1 km from the island to 7.0 individuals \cdot km⁻¹ (95% CI = 5.0 to 10.0) at distances >220 km. The latter can be considered the “pelagic baseline” (i.e., in the absence of colony distance effects) and is similar to the mean relative density reported previously for flying fish in the Caribbean [7.9 individuals \cdot km⁻¹ (29)]. Applying more conservative, simultaneous CIs, the extent of the prey-depleted zone was 154 km (*SI Appendix, Fig. S3*), which can be regarded as the minimum detectable radius of Ashmole’s halo in the current system. Distance from the colony did not affect the frequency of flying fish patches

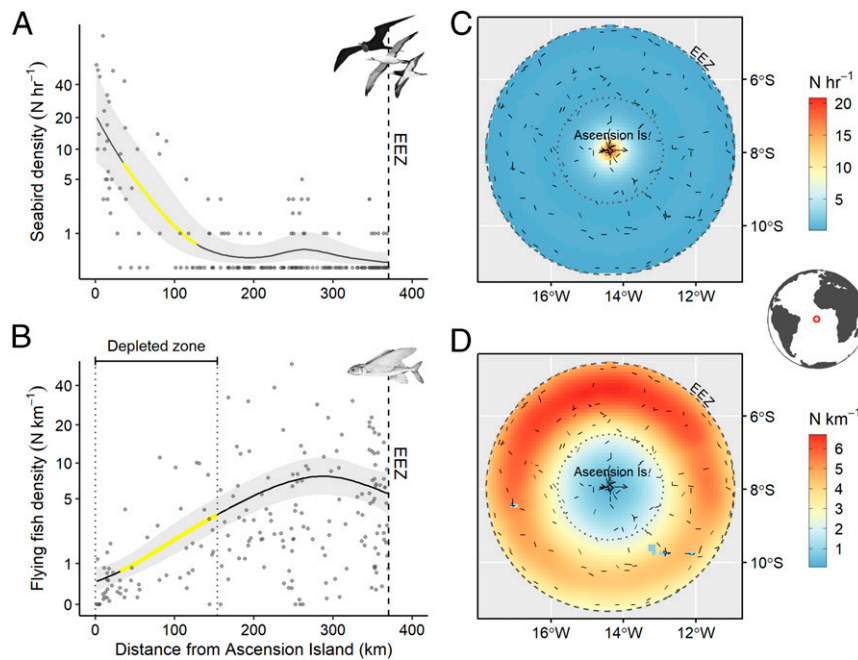


Fig. 1. Direct evidence of “Ashmole’s halo” at Ascension Island. (A and B) Relationship between distance traveled from the Island and relative densities of (A) large-bodied seabirds and (B) their flying fish prey in 192 vessel-based surveys carried out between 2016 and 2019 (note the log scales). Regression lines and shaded polygons represent marginal smooths and associated 95% CIs from GAM(M)s controlling for a suite of potentially confounding environmental and noise variables (Table 1). Regions of significant change are highlighted in yellow and are defined as segments of the fitted splines where the 95% simultaneous CIs around the first derivatives do not overlap zero (*SI Appendix, Fig. S3*). The point at which prey abundance stops increasing can be considered the statistically detectable extent of Ashmole’s halo. (C and D) Predicted spatial distributions of seabirds (C) and flying fish (D) within the Ascension Island exclusive economic zone (EEZ) generated from best-fit GAM(M)s (Table 1). Spatial predictions were generated on a $0.1^\circ \times 0.1^\circ$ grid using mean values of environmental covariates for each cell calculated across all months represented in our survey dataset (methodological covariates were fixed at their means or modes). Survey transects are marked as black lines. The extent of Ashmole’s halo as defined in B is overlaid for comparison. The inset globe map shows the geographic location of the study area.

or the overall level of “patchiness” in their distribution (*SI Appendix, Fig. S6 and Table S7*). However, patches located closer to the colony tended to be smaller and less dense, which together drove the overall declining trend in abundance (*SI Appendix, Fig. S6*).

Other environmental covariates tested were poor predictors of seabird foraging distributions—which supports the findings of a previous telemetry study at Ascension Island (31)—while only

bathymetry and sea surface temperature (SST) contributed additionally to predicting flying fish abundance (Table 1 and *SI Appendix, Figs. S4 and S5*). Flying fish were less abundant in areas of lower SST and over shallow bottom topography (Ascension shelf and seamounts), which is consistent with known habitat preferences in these oceanic species (32). The prey halo we observed can therefore be decomposed into a localized

Table 1. Summary of GAM(M)s fit to vessel-based counts of pelagic seabirds and their flying fish prey

Variable	Flying fish				Seabirds					
	χ^2	P	e.d.f.	Δ DE (%)	χ^2	P	e.d.f.	Δ DE (%)		
Colony distance	106.2	<0.001***	3.08	23.4	186.8	<0.001***	4.48	61.8		
Transect length	34.5	<0.001***	3.19	7.4	—	—	—	—		
Bathymetry	24.7	<0.001***	1.00	5.5	—	—	—	—		
Swell direction*	14.9	<0.001***	2.00	4.1	—	—	—	—		
SST	8.6	0.003**	1.00	2.4	—	—	—	—		
Observer	—	—	—	—	13.8	<0.001***	2.62	4.7		
		DE (%) = 43.6					DE (%) = 69.7			
		R^2 adjusted = 0.12					R^2 adjusted = 0.47			

Significant predictors were identified from a set of 14 methodological and environmental covariates by forward stepwise selection. Results are presented as approximate *P* values from Wald-like tests (χ^2) along with the estimated degrees of freedom (e.d.f.) and change in percentage deviance explained (Δ DE) when the term is excluded from the model. The adjusted R^2 and overall percentage of null deviance explained by each model is also shown (note that DE for individual terms is not expected to sum to the model DE due to the nonorthogonal nature of predictors). Plots of the marginal effects of each term on the response are provided in *SI Appendix, Fig. S5*.

*Affects survey vessel heave and thus the likelihood of disturbing schools into flight.

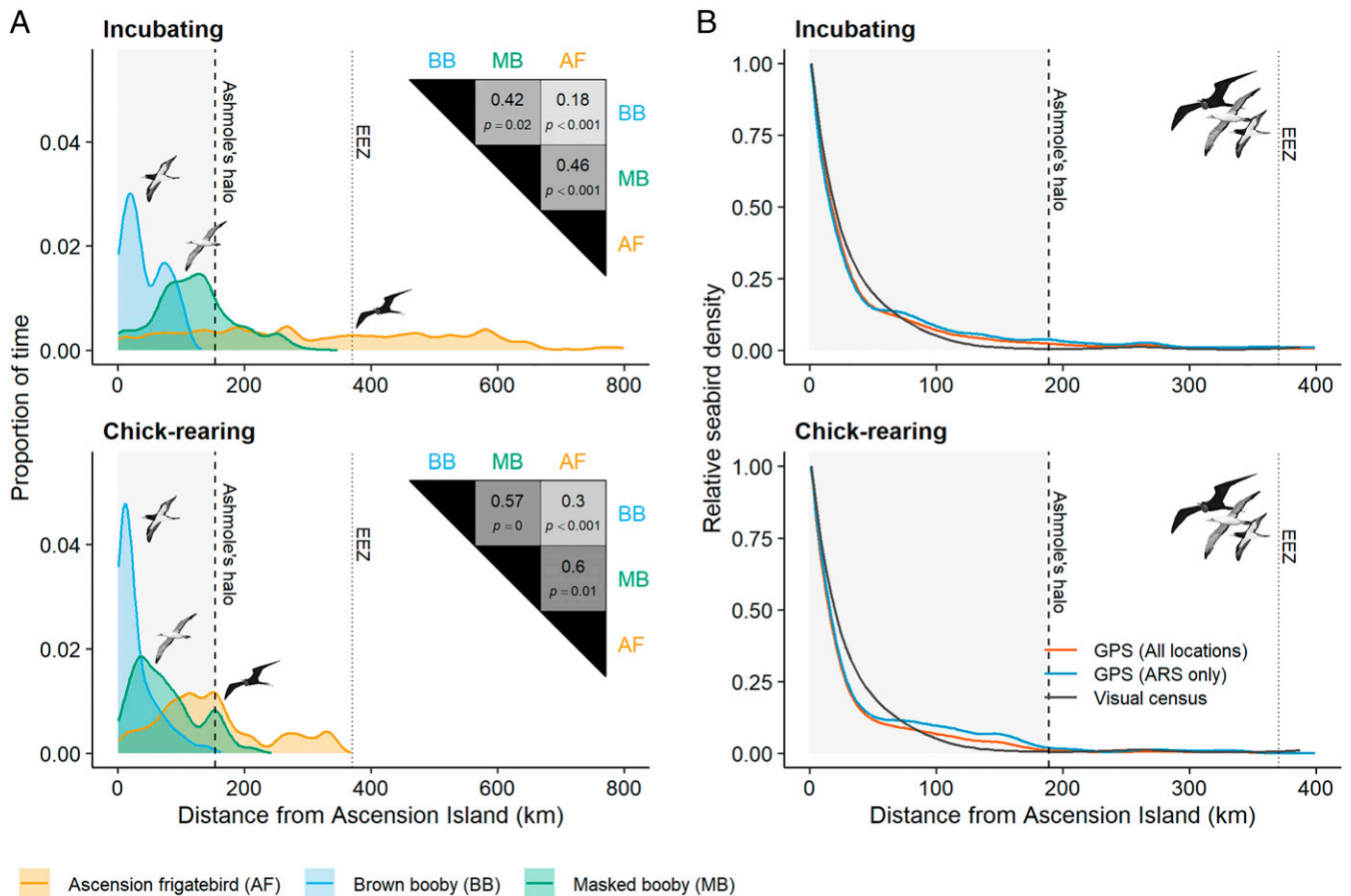


Fig. 2. Foraging distributions of large-bodied seabirds along a colony distance gradient based on GPS telemetry of nesting individuals tagged at Ascension Island. (A) KDEs of the time engaged in ARS behavior at different distances from the colony for each species and breeding stage. The inset triangular matrices show the estimated pairwise niche overlaps and permuted P values. The maximum extent of the observed prey halo (Fig. 1) and the limit of the Ascension Island exclusive economic zone (EEZ) are also shown. (B) Trends in the overall density of large-bodied seabird species as a function of distance from Ascension Island based on GPS and visual census data. KDEs of tracked birds in A were converted to relative densities by dividing by the area of foraging habitat available at each distance increment and merged using a population-weighted mean. Densities were calculated using either complete tracks or only locations associated with ARS behavior, and the resulting distributions were compared with the marginal smooth from a GAMM fitted to vessel-based counts (Fig. 1A).

bathymetric effect and a more extensive colony distance effect that can only be adequately explained by the opposing trend in seabird density (SI Appendix). As with any mid-trophic prey exploited by seabirds, there are numerous nonavian predators of flying fish present in the waters around Ascension (dorado, tuna, billfish, dolphins, etc.); however, these other predators are not obligate central-place foragers and are not expected to differentially deplete prey along a distance gradient. The fact that the distance from seamounts was not a significant predictor of flying fish abundance after controlling for other model terms (GAM: $P = 0.25$) supports this assertion. These seamounts are similar environments to Ascension Island in terms of their shallow depths, abrupt bottom topographies, and associated aggregations of large, pelagic fish but differ conspicuously in the absence of nesting seabirds.

After controlling for significant model terms, there was considerable unexplained variation in flying fish densities, much of which can likely be attributed to their patchy underlying distribution (SI Appendix, Fig. S2) (29, 32). Such sampling error is common in at-sea counts of marine vertebrates and can mask even strong trends in abundance (33), making the prey gradient we demonstrate all the more remarkable. While it is possible that environmental predictors that could help to explain the distribution of prey patches were overlooked, residuals from the flying fish distribution model exhibited no detectable geographic

pattern (Moran's I , $P = 0.51$; SI Appendix) and were not significantly correlated with residual seabird densities (Pearson's $r = 0.01$, degrees of freedom = 190, $P = 0.89$), indicating that seabirds were not locally more abundant in patches of high prey density once the effects of colony distance were controlled for. Given that many tropical seabirds feed by associating with predatory fish and cetaceans (34, 35), background prey abundance may be a relatively poor indicator of prey availability. Nevertheless, our findings support the hypothesis that tropical oceanic seabirds forage in patchy and spatially unpredictable preyscapes (36), where distance from the colony provides the most reliable information on prey encounter rates.

Individual Foraging Behavior, Competition, and the Geometry of Central-Place Foraging. Further insights into the mechanism by which Ashmole's halo forms can be gained by examining how individual breeding seabirds allocate their foraging effort at different distances from the colony (and, hence, at different points along the observed prey gradient) (Fig. 2). Two relevant observations can be derived from these movement data. First, each of the three seabird species that dominate the guild of large-bodied flying fish predators on Ascension Island occupy distinct spatial niches when measured along a colony distance axis: Brown boobies preferentially forage closest to the Island, masked boobies at intermediate distances, and Ascension frigatebirds exploit the

most distant sites (Fig. 2A; overlap: 18 to 60%; all permuted $P < 0.02$). This separation is maintained across breeding stages—despite all species shifting their foraging distributions closer to shore during chick-rearing periods when provisioning requirements limit available foraging time—and may serve to reduce interspecific competition for limiting shared prey resources.

Second, across their respective niches, individual colony members spend comparatively little time foraging adjacent to the island where prey densities are lowest and instead focus their effort further offshore. However, because this effort is distributed over an increasingly large area as distance from the colony increases, the cumulative foraging time per unit area (a proxy for density, or “competition”) decreases monotonically with distance from the colony in a way that is highly consistent with direct density estimates derived from vessel-based surveys (Fig. 2B). This geometric dilution of effort is a key mechanism by which competition is relaxed and higher prey encounter rates are achieved by foraging at more distant sites with higher travel costs, resulting in similar marginal returns across foraging locations (13) (see ref. 37 for a similar discussion on dispersal around communal passerine roosts). Importantly, tracking of breeding individuals constrained to the colony serves to validate seabird foraging distributions inferred from vessel-based surveys and demonstrates that both predator density and foraging intensity exhibit the expected, inverse relationship with prey density predicted by Ashmole’s hypothesis.

Prey Depletion or Prey Displacement? Ashmole (7) envisaged that prey halos form because seabirds directly deplete the resources surrounding their colonies. However, subsequent theoretical studies have shown that similar halos readily emerge from predator evasion and avoidance models, in which prey are either displaced outwards [or deeper (17, 18)] by more frequent attacks closer to the colony (6) or take more strategic decisions on how to distribute themselves based on perceived predation risk (38). These mechanisms are not mutually exclusive, and disentangling them is challenging because the expected impacts on prey densities are identical. Some support for the hypothesis that seabirds deplete their prey base has been derived from bioenergetic models revealing the considerable quantities of food that large colonies require to sustain themselves (19, 39, 40). However, for Ashmole’s halo to form through exploitation alone, the rate of prey capture

around the colony must exceed the rate of replacement through immigration (and recruitment over longer time scales). For highly mobile pelagic prey, like flying fish, local predation effects may therefore be swamped by exchange with surrounding prey-rich areas (41, 42). In evasion/avoidance models, the impact of predators on prey distribution is enhanced by high prey mobility (42). However, the formation of Ashmole’s halo by evasion is expected to be disrupted by the presence of nonavian predators (6)—of which there are many for flying fish—while avoidance models assume that prey have access to reliable cues for predicting predator abundance across hundreds of kilometers of open ocean (38).

To determine whether prey depletion constitutes a viable mechanism, we assessed whether Ascension’s larger breeding seabirds consume enough flying fish to generate the observed prey halo in the absence of any predator avoidance responses (i.e., when prey merely disperse at random). Using a simple bioenergetic model, we estimate that the ca. 24,000 masked boobies, brown boobies, and Ascension frigatebirds reported by Ratcliffe et al. (25) at peak nesting, plus their dependent chicks, require in the order of 10.7 tons of flying fish per day—equivalent to ~38 million fish over a typical 5- to 7-mo breeding cycle (SI Appendix). This is comparable to prey requirements estimated previously for similarly sized seabird colonies (19, 39). When distributed over the foraging range of each species according to the proportion of time spent foraging at different distances from the colony, overall consumption rates range from $0.2 \text{ fish} \cdot \text{km}^{-2} \cdot \text{d}^{-1}$ at 200 km from the island to $10.5 \text{ fish} \cdot \text{km}^{-2} \cdot \text{d}^{-1}$ at 1 km (or 40 to 1,850 $\text{fish} \cdot \text{km}^{-2}$ over a complete breeding cycle).

Our survey method does not allow us to directly estimate absolute flying fish densities. However, if we apply the empirically determined fraction of 20% of fish disturbed into flight within 25 m of the survey vessel estimated previously (43), mean population density beyond the prey-depleted zone (>220 km) can be calculated as $1,400 \text{ fish} \cdot \text{km}^{-2}$ (95% CI: 992 to 2,000). When the above consumption rates and initial population densities are introduced into a simple diffusion model, halos of prey depletion similar to the one we observed can be shown to form around the colony within a single breeding season under realistic levels of random prey dispersal (Fig. 3). Observed prey densities around the colony were lower than those predicted by the model (Fig. 3); however, our estimates of flying fish consumption rates are approximate only and probably underestimate the colony’s

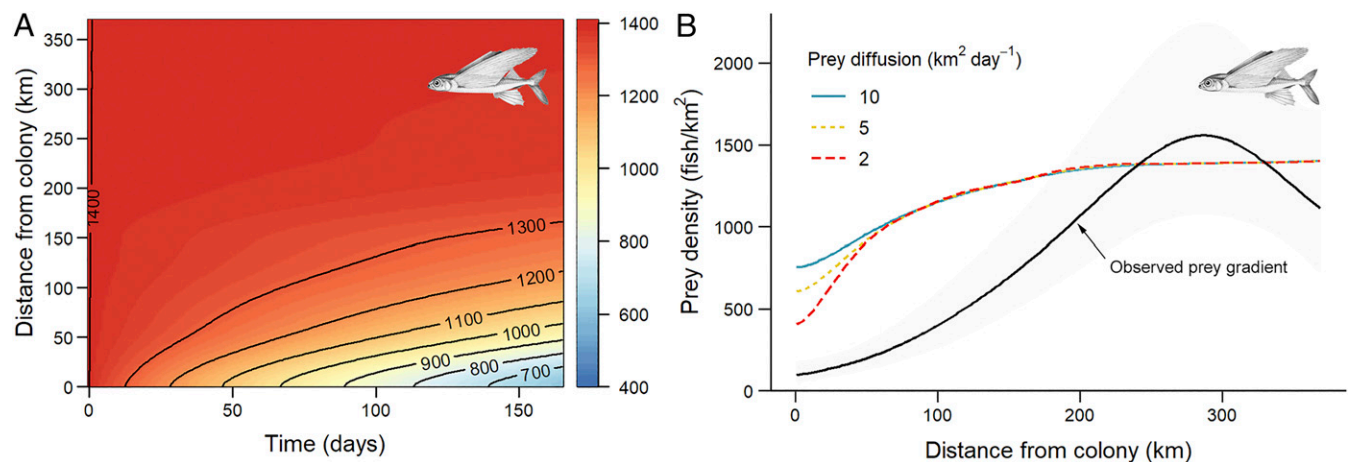


Fig. 3. The evolution of a prey halo around a centrally located seabird colony modeled using a simple consumption–dispersion model. (A) Change in flying fish density at different distances from the colony over a typical breeding season (~165 d) when initial population density is set to the “pelagic baseline” from at-sea surveys (i.e., mean density beyond the maximum extent of the prey-depleted zone: >220 km); daily consumption rates are set based on the estimated prey requirements and foraging distributions of Ascension’s large-bodied breeding seabirds and assuming a prey diffusion coefficient of $D = 5 \text{ km}^2 \cdot \text{d}^{-1}$ (equivalent to mean displacement of $4.5 \text{ km} \cdot \text{d}^{-1}$). (B) Trends in prey density with distance from the colony after the model has run for 165 d with varying rates of prey diffusion. The observed prey gradient modeled from ship-based counts and its associated 95% CI are overlaid for comparison (black line and shaded form, respectively; Fig. 1B).

true prey requirement (*SI Appendix*). With more reliable parameter estimates, the approach we describe could be used to more confidently disentangle the contributions of different mechanisms. Nevertheless, our simulations based on best available data suggest that, even with mobile prey, direct exploitation alone can be sufficient to produce Ashmole's halo.

Implications for Seabird Demography and Pelagic Ecosystem Structure.

Although we cannot conclusively differentiate between alternative causal mechanisms, the ecological outcome of Ashmole's halo for colonial breeders is the same. Numerous studies have shown that as predator colonies grow, individual foraging ranges increase (21); marginal energy gains, provisioning rates, diet quality, and fledging success decrease (6, 20, 21, 44); and population growth slows (6), all of which can be explained in the context of gradients of increased competition and reduced prey availability surrounding the colony. At present, populations of Ascension's larger breeding seabirds are growing rapidly following an eradication of feral cats in 2006 and do not yet appear to be approaching historical carrying capacities set by prey availability (25). Nevertheless, masked boobies nesting at Ascension currently engage in longer foraging trips and have lower fledging success than conspecifics breeding on the neighboring island of St. Helena (1,100 km southeast) where the seabird population is considerably smaller, suggesting that localized prey depletion may already be affecting their behavior and demographic rates (21). As Ascension's seabirds continue to recover, we expect a further expansion of Ashmole's halo to occur, driving long-term declines in individual productivity.

In addition to regulating colony population dynamics, prey depletion halos around pelagic predator colonies also have interesting implications for marine ecosystems more generally. Several recent studies have shown how, by concentrating nutrients gathered over large areas of ocean, seabird colonies can indirectly alter the ecology of adjacent reef systems (45). Here, we show how these same foraging footprints affect the surrounding offshore ecosystem. Direct impacts on forage fish abundance can be detected far from the colony and are likely to extend more broadly through food webs via indirect ecosystem effects. Flying fish, for example, are important mid-trophic species in oceanic food webs that are exploited by numerous epipelagic predators in addition to seabirds (34). How prey depletion around seabird colonies affects the distributions of these other predators, which are not subject to the same spatial constraints, would be an area of considerable interest for further work.

Conclusions

Our results provide a direct demonstration of "Ashmole's halo" in a pelagic seabird colony and show how aggregations of these marine top predators profoundly influence the oceans that surround them. In many ways, Ascension Island represents the idealized case of a single, centrally placed colony lying in a relatively uniform environment, and we would not necessarily expect similarly well-defined prey halos to form around all predator aggregations [e.g., where neighboring colonies interact (14)]. Nevertheless, our results provide much-needed empirical support for a longstanding ecological hypothesis and have clear implications for the management of pelagic ecosystems. In effect, Ashmole's halo constitutes visible evidence of the resource limitation that naturally regulates populations of seabirds and other top predators. It follows that any external pressures that further reduce prey availability within reach of their colonies will have a profound influence on their demographic rates, particularly if they coincide with sensitive reproductive stages. Such reductions may particularly occur when fisheries are added to the competitive landscape, either through direct exploitation of their prey species (46–49) or depletion of the large subsurface predators that many seabirds rely on to locate and catch pelagic prey, including flying

fish (34, 35). Given the scale of the resource footprint we report here, the establishment of large, pelagic marine reserves centered on important seabird nesting islands—such as that recently announced at Ascension Island—would therefore seem to be a justifiable precautionary measure to preserve or restore functioning food webs across the considerable expanses of ocean that these species require to sustain themselves.

Materials and Methods

Seabird Diets. Few studies have examined the diets of seabirds nesting on Ascension, with much of what is known originating from an expedition in the 1950s during which Ashmole conceived his theory of population regulation (26, 28). To supplement this literature with contemporary estimates, we compiled prey inventories from spontaneous regurgitates collected from nesting masked boobies, brown boobies, and Ascension frigatebirds captured for routine population monitoring and tagging studies between 2014 and 2020. Regurgitate data were recorded in different forms by multiple observers and were often not identified to species level. Therefore, we assigned prey items into coarse taxonomic groupings and calculated the frequency of occurrence in the diets of each species based on their presence or absence within the stomach contents of the individuals sampled. For samples where the number of prey items was recorded (or where regurgitates contained only a single identifiable prey type), we also calculated the proportion of the total prey items composed of each taxa (%N). FO and %N were established through identifiable whole or partially digested specimens in regurgitates; we did not attempt to classify undigested hard parts (e.g., squid beaks and fish otoliths).

Predator–Prey Surveys. Simultaneous counts of seabirds and their flying fish prey were conducted between 2016 and 2019 during offshore fishery patrols timed to coincide with the peak tuna longlining season in the region (January to March) (*Dataset S1*). These survey windows also corresponded with seasonal peaks in nesting activity of Ascension's two most numerous large-bodied breeding seabirds (*SI Appendix, Fig. S1*). At the time surveys were carried out, most breeding pairs had completed incubation and were in various stages of chick rearing (masked booby: 89 to 99% chick rearing; Ascension frigatebird: 95 to 99% chick rearing), which is generally the most energetically demanding phase of the annual cycle (50). Counts were performed by one of five observers positioned on the port bow of a 22-m patrol vessel, with two observers being responsible for 87% of surveys. Surveys consisted of linear transects lasting 1 h, during which the vessel attempted to maintain a constant heading and speed (8 kn or ~14.8 km/h). However, changeable sea conditions led to inevitable variation in the total distance traveled. Except for some targeted, distance-stratified sampling within 0 to 50 km of Ascension Island itself, survey locations were selected haphazardly by the position of the patrol vessel at a predetermined start time.

Seabird abundance was estimated using an adaptation of the European Seabirds at Sea protocol (51), which involves counting individuals of each species observed in a strip transect extending from bow to beam and out to a distance of ~300 m (visible to the naked eye with species identifications verified by binoculars where necessary). Relative abundances of flying fish were estimated following Oxenford et al. (29) based on counts of individuals disturbed into flight by the passage of the survey vessel. This method has been widely used for estimating flying fish abundance and is a relevant measure of prey availability for tropical seabirds that naturally feed on flying fish fleeing potential predators at the surface (34). Counts of both taxa were recorded in 5-min sampling intervals and summed across the length of each transect to obtain an overall measure of abundance. To assess the level of spatial aggregation of prey within transects, we computed Lloyd's Patchiness index using the equation $P = 1 + [(\sigma^2 - \mu)/\mu^2]$, where μ and σ^2 are the mean and variance of flying fish counts across successive sampling intervals (52). For each transect, we also computed the number of prey patches encountered, the mean width of prey patches, and the mean density of fish within a patch using the definitions of Oxenford et al. (29), where a patch is defined as a series of contiguous sampling intervals where prey density exceeds the overall median for the study.

We did not apply distance sampling corrections to counts in order to estimate absolute population densities. The vast majority of seabirds were observed in flight, meaning accurate distances were not available, whereas flying fish were only available to count in the narrow swath of disturbed water immediately adjacent to the vessel. Counts are therefore presented as relative abundances standardized by transect length and duration. Detection probability of seabirds and flying fish may be influenced by variation in sea state, visibility, observer bias, and vessel speed (29), and these were statistically controlled for in subsequent analyses.

Species Distribution Models. Ashmole’s hypothesis predicts that densities of seabirds and their prey will vary as opposing functions of distance traveled from the colony. However, a range of other habitat characteristics may influence the distributions of these species and have the potential to obscure or confound expected distance gradients. In order to account for these additional sources of variation, we used GAM(M)s to relate seabird and flying fish counts (N) to a suite of potential environmental predictors while controlling for methodological “noise” variables that may have influenced detectability or observed abundance (see *SI Appendix, Table S5* for covariates and data sources). GAM(M)s were fit using the package “mgcv” (53) for R version 3.6.1 (54) and took the global form:

$$\log(\mu_i) = \alpha + \sum_p f_p(x_{p,i}) + \sum_q \beta_q(x_{q,i}) + \sum_r \zeta_r(x_{r,i}) \quad N_i \sim \text{NegBin}(\mu_i, \theta). \quad [1]$$

f_p is a penalized smooth function (thin plate spline basis) of the p^{th} continuous covariate, β_q is coefficient of the q^{th} parametric term, and ζ_r are random effects. We used raw counts as the response and included distance traveled along each transect as a covariate to standardize survey effort. The response was assumed to follow a negative binomial distribution around the mean (μ) with a dispersion parameter (θ) estimated automatically within the fitting function. Models were developed by forward stepwise selection based on Bayesian approximate P values estimated in *mgcv* using Wald-like tests (55). At each step, we retained the significant term ($P < 0.05$) that most improved the deviance explained. There is no clearly defined concept of “effect size” for smooth terms in GAM(M)s. Results are therefore presented as marginal plots of the effect on the response when other covariates are fixed at their means (continuous) and modal classes (factors) along with an estimate of the change in the proportion of null deviance explained when a model with identical smoothing parameters is refit minus the term of interest. For all influential smooth terms in the model, we also identified the regions of covariate space over which abundance changed significantly by evaluating the first derivatives (i.e., slopes) of the fitted splines and their associated CIs using the R package “gratia” (56). The rate of change at each point evaluated ($n = 100$) was regarded as significant where the 95% CIs of the derivative did not overlap zero. Further details of this method and all model fitting and checking procedures are provided in the *SI Appendix*.

Seabird Tracking. To explore how individual breeding seabirds distribute their foraging effort along the observed prey gradient, we collated GPS tracks from previously published and unpublished studies of Ascension frigatebirds ($n = 32$), masked boobies ($n = 62$), and brown boobies ($n = 17$) tagged at Ascension Island (*SI Appendix, Table S6*). All tracks were collected from nesting individuals tagged during seasonal breeding peaks between September and March and limited to trips occurring within 2 wk of tagging when the breeding stage (incubating or chick rearing) was assumed to be known (21, 31). Tracks were split into 304 discrete foraging trips and interpolated to constant 5-min intervals as described previously (21, 31). Hidden Markov Models were then used to identify phases of “area-restricted search” behavior (ARS) based on flight speed, tortuosity, and altitude (see *SI Appendix* for details). Subsequent analytical steps were run twice: once including all locations and once retaining only locations associated with ARS behavior.

For each tracked individual, we used one-dimensional kernel density estimation (KDE) to estimate the probability of being located within 2-km increments from the colony across all foraging trips, setting the bandwidth equal to the average radius of ARS (57). This is equivalent to the proportion of time spent for a regularly sampled track. Individual KDEs were then averaged by species and breeding stage to obtain the mean proportion of time spent at each distance increment for the tagged population (\bar{P}_d):

$$\bar{P}_d = \frac{\sum_{i=1}^n P_{d,i}}{n} \quad [2]$$

$P_{d,i}$ is the proportion of time spent at distance d by the i^{th} individual, and n is the number of individuals. To test whether tracked cohorts used space differently, we applied the definitions and functions provided by ref. 58 to calculate pairwise niche overlaps between population-level KDEs and performed permutation tests (1,000 iterations) to evaluate the null hypothesis that species occupy the same spatial niche. Niches were regarded as significantly different where <5% of randomly permuted datasets had a kernel

overlap lower than the observed value (i.e., $P < 0.05$) following Benjamini-Hochberg P value adjustment (58).

Population KDEs represent the average proportion of time spent at different distances from the colony but do not account for the area of available foraging habitat over which this effort is distributed. To obtain a measure of cumulative foraging effort that can be compared to vessel-based surveys, population KDEs were therefore divided by the area enclosed by each distance increment (A_d) and normalized to sum to one:

$$D_d = \frac{\bar{P}_d/A_d}{\sum_{d=1}^K \bar{P}_d/A_d} \text{ for } d = 1, \dots, \quad [3]$$

These population-level distributions were then combined to obtain an overall estimate of seabird foraging intensity per unit area (or “density”) at each distance increment from the colony (\bar{D}) by computing the weighted average based on the approximate number of breeding pairs of each species (M):

$$\bar{D}_d = \frac{\sum_{j=1}^n D_{d,j} \times N_j}{n} \quad [4]$$

where $D_{d,j}$ is the foraging intensity of the j^{th} species at distance d , and n is the number of tagged populations.

Estimating Seabird Predation Impacts on Flying Fish Density. Following previous studies (19, 39), we combined approximate, species-specific field metabolic rates and population sizes with reported prey energy densities and assimilation efficiency in seabirds to estimate the mean daily prey requirement of Ascension’s seabirds during seasonal breeding peaks (*SI Appendix and Dataset S2*). We then distributed this catch across the foraging range of each species by multiplying by the proportion of time spent foraging at each distance increment from the colony (Eq. 2) to estimate the number of fish consumed/km²/day (Q , the consumption rate). The rate of change in prey population density (N) at each radial distance from the colony (r) was then estimated using the following one-dimensional diffusion-reaction model:

$$\frac{\partial N}{\partial t} = \frac{1}{A_r} \cdot \frac{\partial}{\partial r} \left(A_r \cdot D \cdot \frac{\partial N}{\partial r} \right) - Q, \quad [5]$$

where t is the time in days, D is the diffusion coefficient (a measure of prey mobility), and $A_r = 2\pi r$ is the length of the interface across which dispersion can occur. The model states that the rate of change in prey population density at distance r depends on net immigration (which is a function of the local steepness of the prey gradient and the diffusion coefficient) minus the continuous rate of consumption. The model was initiated at $t = 0$ with a uniform $N = 1,400$ fish/km² (see *Results and Discussion*). Boundary conditions (i.e., values at the edge of the model) were set at $N_{r=370} = 1,400$ for the downstream boundary (i.e., the limit of our prey surveys) and $\frac{\partial N}{\partial r} = 0$ for the upstream boundary (i.e., no prey exchange where colony distance is zero). We then ran the model over a 165-d period [the minimum duration of a breeding cycle for boobies and frigatebirds on Ascension Island (28)] using the R package “ReacTran” (59) to examine how prey density evolves under different diffusion rates (*Dataset S2*).

Data Availability. Raw seabird and flying fish counts from at-sea surveys and associated environmental variables are available in *Dataset S1*. Seabird tracking data are available on request via the BirdLife International Seabird Tracking Database (<http://seabirdtracking.org/>). Example code used for the consumption–dispersion model is available in *Dataset S2*.

ACKNOWLEDGMENTS. This work was cofunded by the UK Government’s Conflict, Security, and Stability Fund and by a Darwin Initiative grant (ref. DPLUS063) awarded to the Ascension Island Government and other partners. We are indebted to the master and crew of the St. Helena fishing vessel *M/V Extractor* who supported all aspects of the offshore fieldwork. We also wish to thank Rob Mrowicki and the late Katie Downes, who participated in some at-sea surveys, as well as Sophie Tuppen, Tess Handby, Elizabeth Mackley, Kenickie Andrews, Nathan Fowler, Derren Fox, Jolene Sim, Julia Sommerfeld, Annalea Beard, and Pete Mayhew who all contributed to past seabird tagging projects on Ascension Island.

1. E. L. Preisser, D. I. Bolnick, M. F. Benard, Scared to death? The effects of intimidation and consumption in predator–prey interactions. *Ecology* **86**, 501–509 (2005).
 2. E. L. Preisser, D. I. Bolnick, The many faces of fear: Comparing the pathways and impacts of nonconsumptive predator effects on prey populations. *PLoS One* **3**, e2465 (2008).

3. S. L. Lima, Nonlethal effects in the ecology of predator–prey interactions. *Bioscience* **48**, 25–34 (1998).
 4. J. A. Estes *et al.*, Trophic downgrading of planet Earth. *Science* **333**, 301–306 (2011).
 5. J. K. Baum, B. Worm, Cascading top-down effects of changing oceanic predator abundances. *J. Anim. Ecol.* **78**, 699–714 (2009).

6. S. Lewis, T. N. Sherratt, K. C. Hamer, S. Wanless, Evidence of intra-specific competition for food in a pelagic seabird. *Nature* **412**, 816–819 (2001).
7. N. P. Ashmole, The regulation of numbers of tropical oceanic birds. *Ibis* **103b**, 458–473 (1963).
8. R. W. Furness, T. R. Birkhead, Seabird colony distributions suggest competition for food supplies during the breeding season. *Nature* **311**, 655–656 (1984).
9. C. E. Kuhn, J. D. Baker, R. G. Towell, R. R. Ream, Evidence of localized resource depletion following a natural colonization event by a large marine predator. *J. Anim. Ecol.* **83**, 1169–1177 (2014).
10. P. Salo, P. B. Banks, C. R. Dickman, E. Korpimäki, Predator manipulation experiments: Impacts on populations of terrestrial vertebrate prey. *Ecol. Monogr.* **80**, 531–546 (2010).
11. D. K. Cairns, “Population regulation of seabird colonies” in *Current Ornithology*, D. M. Power, Ed. (Springer US, 1992), pp. 37–61.
12. V. Birt, T. Birt, D. Goulet, D. Cairns, W. Montevecchi, Ashmole’s halo: Direct evidence for prey depletion by a seabird. *Mar. Ecol. Prog. Ser.* **40**, 205–208 (1987).
13. A. J. Gaston, R. C. Ydenberg, G. E. J. Smith, Ashmole’s halo and population regulation in seabirds. *Mar. Ornithol.* **35**, 119–126 (2007).
14. E. D. Wakefield et al., Space partitioning without territoriality in gannets. *Science* **341**, 68–70 (2013).
15. R. Bonal, J. M. Aparicio, Evidence of prey depletion around lesser kestrel *Falco naumanni* colonies and its short term negative consequences. *J. Avian Biol.* **39**, 189–197 (2008).
16. K. L. Wilson et al., Social–ecological feedbacks drive spatial exploitation in a northern freshwater fishery: A halo of depletion. *J. Appl. Ecol.* **57**, 206–218 (2020).
17. D. G. Ainley, R. G. Ford, E. D. Brown, R. M. Suryan, D. B. Irons, Prey resources, competition, and geographic structure of kittiwake colonies in prince william sound. *Ecology* **84**, 709–723 (2003).
18. D. G. Ainley et al., Trophic cascades in the western ross sea, Antarctica: Revisited. *Mar. Ecol. Prog. Ser.* **534**, 1–16 (2015).
19. K. H. Elliott et al., Central-place foraging in an Arctic seabird provides evidence for storer-ashmole’s halo. *Auk* **126**, 613–625 (2009).
20. L. T. Ballance, D. G. Ainley, G. Ballard, K. Barton, An energetic correlate between colony size and foraging effort in seabirds, an example of the Adélie penguin *Pygoscelis adeliae*. *J. Avian Biol.* **40**, 279–288 (2009).
21. S. Oppel et al., Foraging distribution of a tropical seabird supports Ashmole’s hypothesis of population regulation. *Behav. Ecol. Sociobiol.* **69**, 915–926 (2015).
22. G. L. Hunt, Z. A. Eppley, D. C. Schneider, Reproductive performance of seabirds: The importance of population and colony size. *Auk* **103**, 306–317 (1986).
23. R. Jovani et al., Colony size and foraging range in seabirds. *Oikos* **125**, 968–974 (2016).
24. D. G. Ainley, G. Ballard, K. M. Dugger, Competition among penguins and cetaceans reveals trophic cascades in the western Ross Sea, Antarctica. *Ecology* **87**, 2080–2093 (2006).
25. N. Ratcliffe et al., The eradication of feral cats from Ascension Island and its subsequent recolonization by seabirds. *Oryx* **44**, 20 (2010).
26. B. Stonehouse, Ascension island and the British ornithologists union centenary expedition 1957–59. *Ibis* **103**, 107–123 (1962).
27. B. Stonehouse, S. Stonehouse, The frigate bird *Fregata aquila* of Ascension Island. *Ibis* **103**, 409–422 (1963).
28. D. F. Dorward, Comparative biology of the white booby and the brown booby *Sula* spp. at Ascension. *Ibis* **103**, 174–220 (1962).
29. H. A. Oxenford, R. Mahon, W. Hunte, Distribution and relative abundance of flyingfish (Exocoetidae) in the eastern Caribbean. I. Adults. *Mar. Ecol. Prog. Ser.* **117**, 11–23 (1995).
30. B. Stonehouse, The tropic birds (genus *Phaethon*) of Ascension Island. *Ibis* **103**, 124–161 (1962).
31. S. Oppel et al., Seasonal shifts in foraging distribution due to individual flexibility in a tropical pelagic forager, the Ascension frigatebird. *Mar. Ecol. Prog. Ser.* **585**, 199–212 (2017).
32. J. Churnside et al., Surveying the distribution and abundance of flying fishes and other epipelagics in the northern Gulf of Mexico using airborne lidar. *Bull. Mar. Sci.* **93**, 591–609 (2017).
33. B. L. Taylor, M. Martinez, T. Gerrodette, J. Barlow, Y. N. Hrovat, Lessons from monitoring trends in abundance of marine mammals. *Mar. Mamm. Sci.* **23**, 157–175 (2007).
34. D. W. Au, R. L. Pitman, Seabird interactions with dolphins and tuna in the eastern tropical Pacific. *Condor* **88**, 304–317 (1986).
35. S. Maxwell, L. Morgan, Foraging of seabirds on pelagic fishes: Implications for management of pelagic marine protected areas. *Mar. Ecol. Prog. Ser.* **481**, 289–303 (2013).
36. H. Weimerskirch, Are seabirds foraging for unpredictable resources? *Deep Sea Res. Part II Top. Stud. Oceanogr.* **54**, 211–223 (2007).
37. W. J. Hamilton, W. M. Gilbert, Starling dispersal from a winter roost. *Ecology* **50**, 886–898 (1969).
38. L. Hemerik, M. V. Opheusden, R. Ydenberg, Ashmole’s halo as the outcome of a predator-prey game. *Mar. Ornithol.* **42**, 125–136 (2014).
39. H. Weimerskirch, M. Le Corre, C. Bost, Foraging strategy of masked boobies from the largest colony in the world: Relationship to environmental conditions and fisheries. *Mar. Ecol. Prog. Ser.* **362**, 291–302 (2008).
40. R. W. Furness, Energy requirements of seabird communities: A bioenergetics model. *J. Anim. Ecol.* **47**, 39–53 (1978).
41. A. Sih, D. E. Wooster, Prey behavior, prey dispersal, and predator impacts on stream prey. *Ecology* **75**, 1199–1207 (1994).
42. S. D. Cooper, S. J. Walde, B. L. Peckarsky, Prey exchange rates and the impact of predators on prey populations in streams. *Ecology* **71**, 1503–1514 (1990).
43. G. V. Zuyev, V. N. Nikol’skiy, Procedure for the quantitative recording of flyingfishes (Exocoetidae). *J. Ichthyol.* **20**, 147–149 (1980).
44. M. G. Forero, J. L. Tella, K. A. Hobson, M. Bertelotti, G. Blanco, Conspecific food competition explains variability in colony size: A test in magellanic penguins. *Ecology* **83**, 3466–3475 (2002).
45. N. A. J. Graham et al., Seabirds enhance coral reef productivity and functioning in the absence of invasive rats. *Nature* **559**, 250–253 (2018).
46. C. Barbraud et al., Density dependence, prey accessibility and prey depletion by fisheries drive Peruvian seabird population dynamics. *Ecography* **41**, 1092–1102 (2018).
47. D. Grémillet et al., Persisting worldwide seabird-fishery competition despite seabird community decline. *Curr. Biol.* **28**, 4009–4013.e2 (2018).
48. S. Bertrand et al., Local depletion by a fishery can affect seabird foraging. *J. Appl. Ecol.* **49**, 1168–1177 (2012).
49. R. W. Furness, “Competition between fisheries and seabird communities” in *Advances in Marine Biology*, J. H. S. Blaxter, F. S. Russell, M. Yonge, Eds. (Academic Press, 1982), pp. 225–307.
50. R. H. Drent, S. Daan, The prudent parent: Energetic adjustments in avian breeding 1). *Ardea* **68**, 225–252 (1980).
51. K. C. Camphuysen, S. Garthe, Recording foraging seabirds at sea: Standardised recording and coding of foraging behaviour and multi-species foraging associations. *Atlant. Seabirds* **6**, 1–32 (2004).
52. M. Lloyd, Mean crowding. *J. Anim. Ecol.* **36**, 1–30 (1967).
53. S. N. Wood, Fast stable restricted maximum likelihood and marginal likelihood estimation of semiparametric generalized linear models. *J. R. Stat. Soc. Series B Stat. Methodol.* **73**, 3–36 (2011).
54. R Core Team, R: A language and environment for statistical computing (version 3.6.1, R Foundation for Statistical Computing, 2020).
55. S. N. Wood, On p-values for smooth components of an extended generalized additive model. *Biometrika* **100**, 221–228 (2013).
56. G. L. Simpson, Gratia: Graceful ‘Ggplot’-Based Graphics and Other Functions for GAMs Fitted using “mgcv” (R package version 0.4.1, 2020). <https://CRAN.R-project.org/package=gratia>. Accessed 15 June 2021.
57. B. G. Lascelles et al., Applying global criteria to tracking data to define important areas for marine conservation. *Divers. Distrib.* **22**, 422–431 (2016).
58. S. Geange, S. Pledger, K. Burns, J. Shima, A unified analysis of niche overlap incorporating data of different types. *Methods Ecol. Evol.* **2**, 175–184 (2011).
59. K. Soetaert, F. Meysman, Reactive transport in aquatic ecosystems: Rapid model prototyping in the open source software R. *Environ. Model. Softw.* **32**, 49–60 (2012).